RESEARCH PAPER

Nano Science and Technology Journal 2(1) 30-40 March 2024

Investigation of the Properties and Applications of Nano Structured Silver Thin Films in Enhancing the Performance of Water and Wastewater Treatment Systems

Vahed adeshteh[1], Saeid Sarabadani[1], Maryam Nasehnejad[1]*, Zahra Rastin[1]

[1]*Markazi Province Water and Wastewater Company, Arak, Iran*

Article History:
Received 07 June 2025
Accepted 26 July 2025
Published 15 August 2025

Keywords:
Silver thin film
Morphology evolution
Dynamic growth exponent
Grain size distribution
Antibacterial activity
Water and wastewater treatment

*Corresponding Authors Email:
m.nasehnejad@gmail.com

DOI: 10.22034/nstj.2025.2063036.1015

Abstract

This study explores the growth behavior, microstructure, and antibacterial performance of electrodeposited silver (Ag) thin films on different substrates, with particular attention to their application in water and wastewater treatment systems. Scanning electron microscopy (SEM) and X-ray diffraction (XRD) analyses reveal that substrate material strongly affects film morphology: Ag films on copper (Cu) show compact granular structures, while those on Au_2PdAg/glass exhibit surface cracks that impair antibacterial effectiveness. XRD patterns confirm the polycrystalline nature of the films with preferential (111) orientation, known for its high surface energy and ion-release efficiency. Crystallite size evolution follows a dynamical scaling law with a growth exponent $\beta \approx 0.67$, indicating anomalous roughness behavior. Log-normal grain size distributions and SEM analyses yield a dynamic exponent of $1/z \approx 0.63$, suggesting three-dimensional cluster growth involving the full cluster surface in mass transport. Increased film thickness leads to higher surface roughness, as confirmed by X-ray reflectivity, which improves hydrophilicity and ion transport. Despite grain growth reducing specific surface area, roughness compensates by enhancing ion release and structural durability. Additionally, film density values obtained from reflectivity are lower than bulk Ag, likely due to porosity and oxidation. These findings underscore the importance of controlling thickness and substrate compatibility to optimize the antibacterial efficiency and stability of Ag thin films for aqueous environments.

1. Introduction

Nanometric thin films are significant in different fields of material science and technology. Most of properties of thin film (such as electronic, optical, mechanical, etc.) change strongly when thin film is formed from bulk material because of the confinement influences. microstructural characteristics of films such as grain size, crystalline structure, surface topography have an important effect on modifying the physical features of the thin films. it drastically is related to deposition technique and growth factors (e.g. time, rate, etc.). In order to control the grain size during growth, the first and most important step in the preparation of high quality films for applications is, unambiguously, the knowledge of the structure of the samples, as well as the control of growth [1, 2].

Silver is a metallic element important in both science and technology. silver films have many practical applications in various fields such as surface-enhanced Raman scattering [3, 4], catalysis [4], sensors [5] nanophotonic [6], superhydrophobicity [7], electrode [8]. There are various techniques for preparing the silver thin films including electrodeposition, molecular-beam epitaxy, sputtering, physical vapor deposition [9- 12]. Electrodeposition method could be a suitable method for the growth of Ag film because of its ability to produce deposits with changeable composition. Other benefits of this economical method include low cost, large area deposition and simplicity in experimental setups.

Thin layers of silver have found important applications in the water and wastewater industry, primarily due to their strong antimicrobial properties and chemical stability. One of the most prominent uses is in the disinfection and sterilization of water. Silver ions are highly effective against a broad spectrum of microorganisms, including bacteria, viruses, and fungi. When applied as a thin film, silver can release ions gradually, providing a long-lasting antimicrobial effect without the need for continuous chemical dosing, such as chlorine. This makes silver-coated surfaces particularly valuable in systems where chemical contamination must be minimized, such as in drinking water treatment or medical water supplies [13, 14]. Another key application is in membrane technology. Thin silver layers are often deposited on filtration membranes used in processes like reverse osmosis or nanofiltration. These coatings help prevent biofouling, a major operational issue caused by the accumulation of microbial films on membrane surfaces. By inhibiting microbial growth, silver layers extend the operational life of membranes, reduce the frequency of cleaning, and enhance overall filtration efficiency [15]. Furthermore, silver coatings are used on the inner surfaces of pipes, tanks, and other infrastructure in water and wastewater systems. These coatings inhibit microbial colonization and biofilm formation, which are common in moist environments and can lead to both health risks and reduced system performance. Silver's chemical inertness also ensures that it does not react with water constituents, thereby maintaining the integrity and safety of the water. In some advanced purification systems, nanostructured silver films are integrated into composite materials or filters to create multifunctional surfaces with both mechanical strength and antimicrobial activity. These systems are increasingly used in both centralized treatment facilities and point-of-use devices, such as household water purifiers [16, 17].

The study of the morphology of such films with the variation of thickness and thermal processes gives an idea about the growth mechanism of these films [18]. Study of morphology and understanding of growth mechanism are, also, essential to fabricate nanostructured materials in a controlled way for desired properties. In fact, such systems are functional materials since their chemical and physical properties are strongly correlated to the structural ones (size, shape, crystallinity, etc.). As a consequence, the necessity to develop bottom-up procedures (in contrast to the traditional top-down scaling scheme) allowing the manipulation of the structural properties of these systems raised. Such studies find a renewed interest today for the potential nanotechnology applications [2, 19]. The key point of such studies is the understanding of the thin film kinetic growth mechanisms to correlate Investigation of the characteristics of the electrodeposited Ag films helps to comprehend their features and applications. in this study, we have reported the growth of Ag thin films prepared by electrodeposition technique. Scanning electron microscopy (SEM) and x-ray reflectivity (XRR) techniques are employed to study the surface evolution of nanometric Ag films. SEM is a significant method for studying surface morphology of the thin films in real space. It can be obtained and processed the images of the top surface which provides information regarding the surface morphology and the change in grain size with respect to the thin film thickness. XRR measurements gives us unique information about the surface roughness and film density.

2. Experimental

The electrolyte bath used for the electrodeposition of silver coatings has the composition: 200 mM silver nitrate ($AgNO_3$, $7H_2O$, ≥99.0% purity, Merck)+ 60 mM boric acid (H_3BO_3, ≥99.5% purity, Sigma-Aldrich) as an additive. All chemicals were of analytical grade and used without further purification. The solution was freshly prepared with water first doubly distilled. The temperature during electrodeposition was maintained at 25 °C and the pH of the solution was adjusted to approximately 2. Electrodeposition was performed galvanostatically (current density of j = 1 $mA.cm^{-2}$) in a dark chamber in a conventional three-electrode cell. The counter electrode was a platinum foil. The reference electrode was a calomel electrode Ag/AgCl electrode and all potentials were referred to it. Working electrodes were Cu and Au_2PdAg /glass.

After deposition of films, deposit morphology was studied by SEM using a LEO instrument model 1455 VP at a 20 KV accelerating voltage. The SEM images were analyzed using the Gatan digital micrograph software. XRR technique is used to study the surface roughness and film density of the deposits. X-ray measurements were carried out using a conventional two-circle X-ray diffractometer (Siemens D-5000) with Cu K_α radiation (λ =0.154 nm) operating at 1.2 kW.

3. Results and discussion

The first, substrate influence on the morphology of thin Ag films was studied. Figure 1 shows SEM images of the Ag films grown on the Cu and Au_2PdAg /glass substrates with the thickness of 150 nm. Morphological analysis showed that the film prepared on the Cu substrate were granular and compact. Moreover, the film electrodeposited on the Au_2PdAg /glass substrate has cracks on the surface. The results indicate that the choice of substrate significantly influences the morphology of the silver thin film, which in turn affects its antibacterial performance. A granular and compact structure increases the effective surface area and promotes a more uniform distribution of silver, leading to a more consistent release of silver ions and consequently a more stable antibacterial effect. In contrast, the presence of surface cracks causes discontinuities in the film, resulting in uneven ion release and reduced antibacterial efficacy. Additionally, these cracks may accelerate film degradation or delamination under humid and chemically aggressive conditions. The exposure of the underlying substrate in cracked areas can further facilitate localized bacterial growth. These findings highlight the importance of designing appropriate thin film structures tailored to the substrate type and operational conditions in water treatment systems.

XRD patterns for the Ag layers with different thicknesses on the Cu substrate are shown in Figure 2. For comparison, the standard diffraction peaks of face-centered cubic (fcc) silver (JCPDS file No. 04–0783) and fcc copper (JCPDS file No. 89-2838) are also included. Several peaks corresponding to the (111), (200), (220), and (311) planes of fcc Ag are observed, confirming the polycrystalline nature of the deposited films. Among them, the (111) peak is the most intense, indicating a preferred orientation along the (111) direction. This observation is consistent with previous studies [13, 20–22], which reported that Ag thin films tend to grow with (111) crystallographic planes parallel to the substrate surface, as this orientation has the lowest surface energy. The preferred (111) peak in the silver thin film structure is recognized as one of the stable crystal planes with relatively high surface energy. This orientation enhances the surface activity of the film, facilitating a more effective release of silver ions (Ag^+), which are the primary agents responsible for antibacterial activity. Moreover, the stable (111) structure increases the resistance of the thin film against corrosion and chemical degradation in harsh environments such as water and wastewater systems [13]. These characteristics contribute to improved performance and prolonged lifespan of water and wastewater treatment systems. The mean crystallite size, S, is determined from the full width at half maximum (FWHM) of the main (1 1 1) peak by applying the Scherrer formula:

$$D = \frac{k\lambda}{\beta cos\theta} \quad (1)$$

where K – the particle shape factor, 0.9, λ – X-ray wavelength, β – the half-width of (hkl) reflection, θ = 2θ/2 – Bragg angle corresponding to (hkl) reflection.

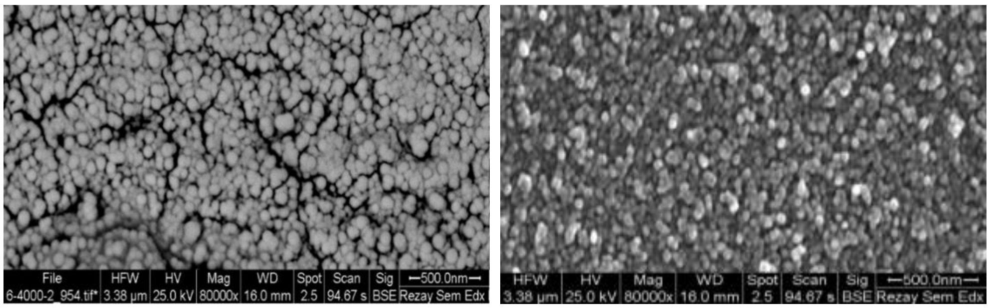

Fig 1. SEM images of the Ag films grown on the (a) Au2PdAg /glass and (b) Cu substrate with the thickness of 150 nm.

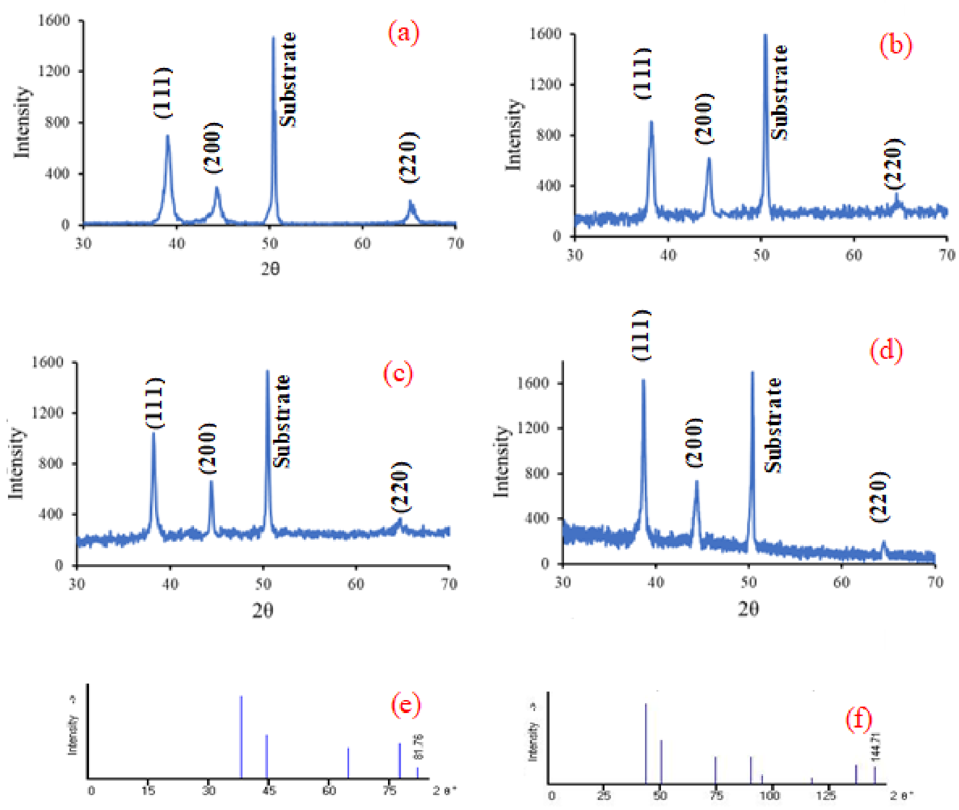

Fig 2. X-ray diffraction spectra for Ag films grown on the Cu substrate with the thickness of (a) 150 nm, (b) 450 nm, (c) 750nm, (d) 900 nm, (e) XRD pattern of standard Ag powder (f) XRD pattern of standard Cu powder.

The growth of thin films is a complex process in which surface properties such as roughness, grain structure, and morphology evolve with time. To model these evolution, the concept of dynamic scaling is used, involving parameters such as the growth exponent (β) and the dynamic exponent (z). The growth exponent (β) quantifies the rate at which surface roughness increases with time, while the dynamic exponent (z) characterizes the nature of the growth mechanism and depends on its specific physical processes [23].

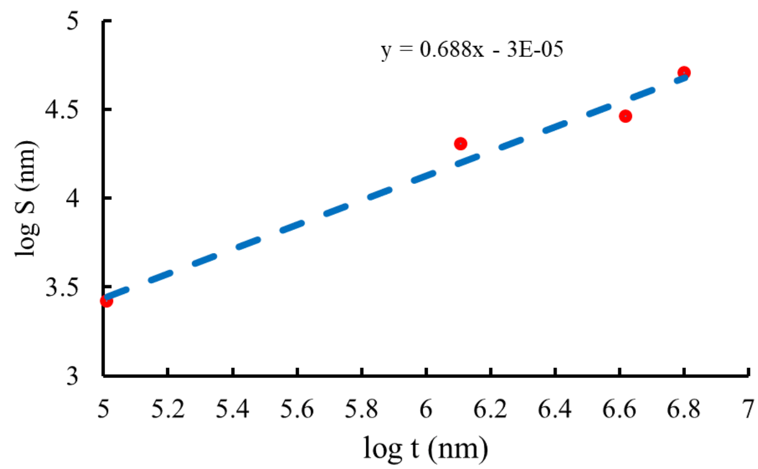

Fig 3. Log–log plot of mean crystallite size in term of film thickness.

The mean crystallite sizes (S) have been represented as a function of the film thickness (t) in figure 3, where they show a good fit to the dynamical scaling law:

$$S \sim t^{\beta} \quad (2)$$

where β is growth exponent. The value of the growth exponent β is obtained 0.67. High β (above 0.25) indicates growth situations which displays anomalous scaling. A value of β = 0.67 indicates a non-normal and nonlinear roughness growth occurring at a rate higher than typical cases. It can be arisen due to non-local effects including bulk diffusion [23]. This behavior can lead to distinctive features on the silver thin film surface, including an increased effective surface area and enhanced release of silver ions, which are critical for improving its antibacterial properties. It can be obtained information about the growth mechanism from the evolution of the film morphology with the film thickness. For this purpose, the Ag films with different thickness (or alternatively time) were electrodeposited on the Cu substrate at room temperature. Figure 4 demonstrates SEM images of these samples. It is observed that Ag films have uniform distribution of grains over the surface in all regions as observed earlier by others in metal films studies [24]. A uniform distribution of silver grains on the surface of thin silver films facilitates a regular and stable release of silver ions, which plays a crucial role in maintaining continuous and uniform antibacterial activity. Such distribution prevents localized concentration of ion release, thereby ensuring consistent antimicrobial performance across the entire film surface. Furthermore, a uniform grain distribution helps reduce the formation of cracks, discontinuities, and stress concentrations, which enhances the durability and stability of the thin film under the harsh environmental conditions typical of water and wastewater treatment systems.

As the thickness film increases, the grains size increases. This result implies that grain size and surface morphology of deposits can easily be controlled using various thicknesses. Smaller grain sizes lead to an increased specific surface area of the silver thin films, providing a greater number of active sites for the release of silver ions (Ag^{+}). These silver ions are the primary agents responsible for antimicrobial properties, and smaller grains typically correspond to a higher ion release rate and enhanced antimicrobial activity. Moreover, uniformly distributed small grains facilitate a more controlled and stable release of ions, contributing to the sustained efficacy of the antimicrobial properties over time. Additionally, finer grains tend to form a more porous structure with smaller pores, which enhances the adsorption of contaminants and improves the filtration of fine particles. On the other hand, the presence of uniform and optimized porosity promotes smoother fluid flow and reduces filter clogging, thereby improving the overall performance of water and wastewater treatment systems. Conversely, larger grains, due to their lower surface-to-volume ratio, are less prone to surface cracks and discontinuities, which results in increased structural uniformity and durability of the film. Larger grains also generally form a mechanically stronger structure with better adhesion to the substrate, enhancing the thin film's resistance to mechanical stress, corrosion, and erosion. Therefore, the selection of grain size should be adjusted according to the application and the specific needs of the treatment system.

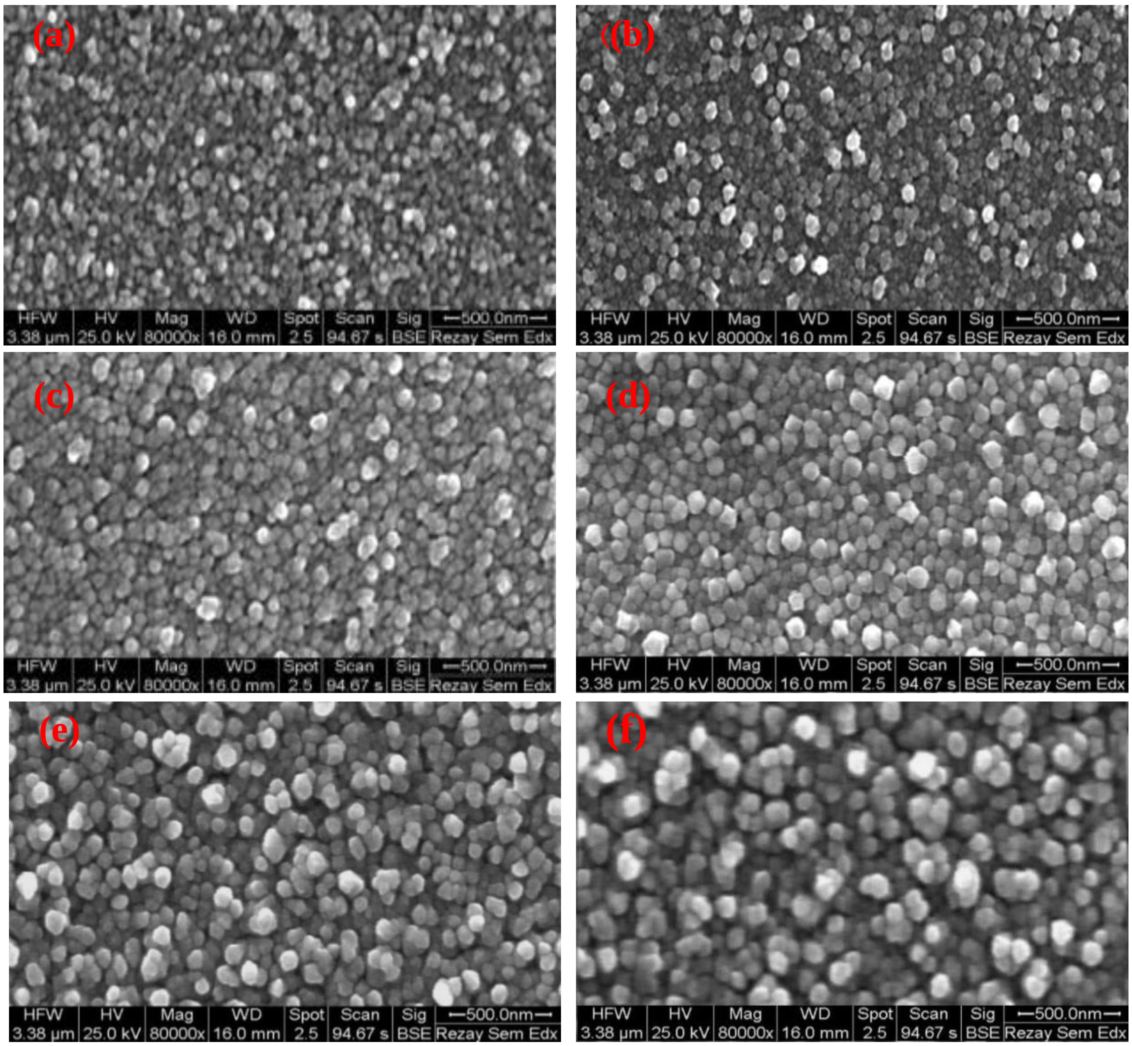

Fig 4. SEM images of Ag films grown on the Cu substrate with the thickness of (a) 150 nm, (b) 300 nm, (c) 450 nm, (d) 600 nm, (e) 750nm, (f) 900 nm.

From the SEM images, the change in morphology of the Ag films versus the film thickness is followed. From such analyses, it can be extracted the grain radius distributions, describing each area of grain by the surface image dividing of a plane which was located at half grain height, by the Gatan software. Therefore, Figure 5 displays the grain size distributions for the deposits presented in Figure 3. Every distribution was computed on a statistical population of 400 grains. It can be fitted the distribution of the grain radius *R* in every film with the log-normal function [25]:

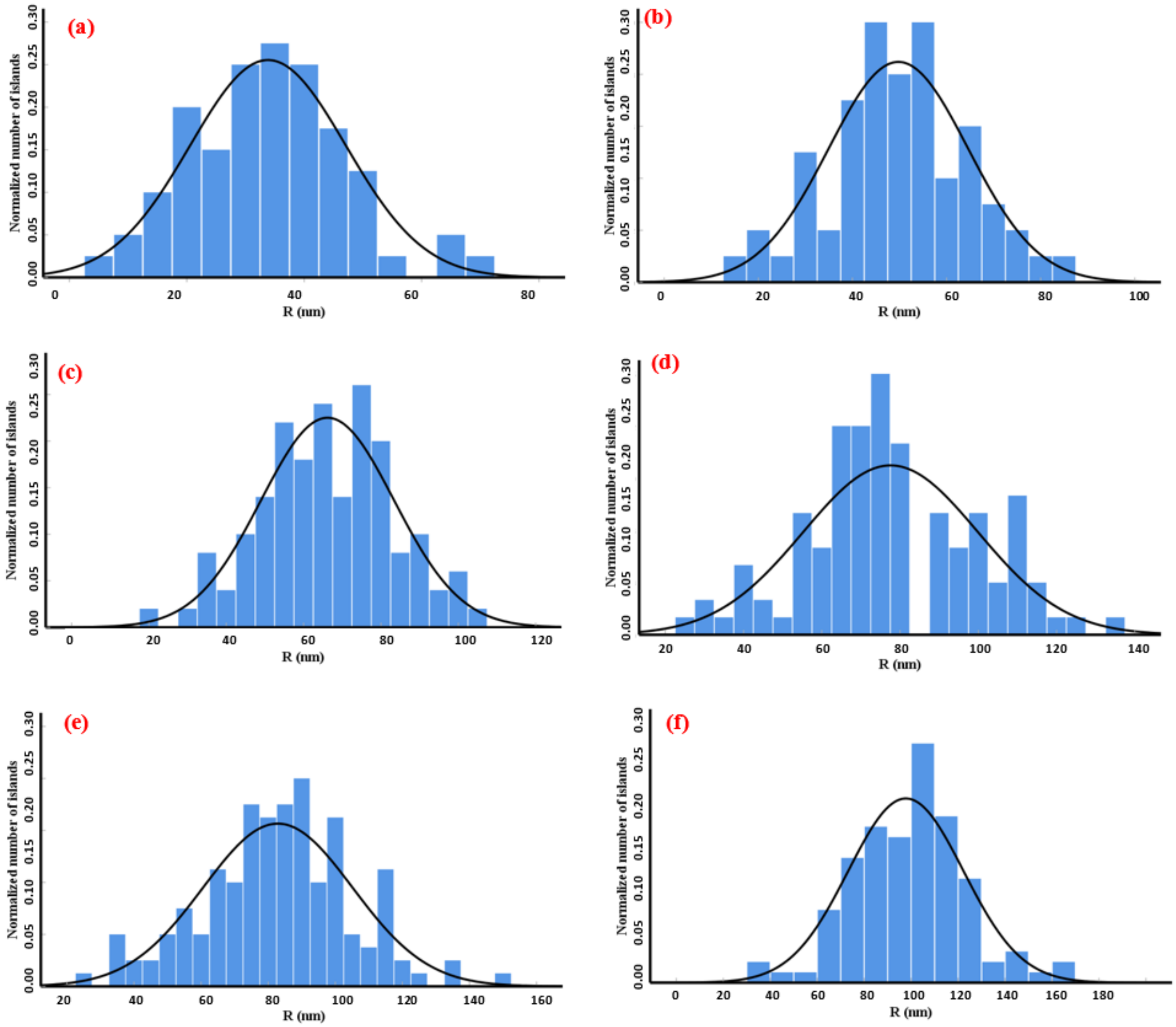

Fig 5. the grain size distributions for the deposits presented in Figure 4.

$$f(D) = \frac{1}{2\sqrt{2\pi}\sigma R} e^{-\frac{ln^2(R/R_C)}{2\sigma^2}} \quad (3)$$

where σ is the standard deviation and R_c indicates the critical radius. The mean radius of the grains is defined as $\langle R \rangle = R_c e^{\frac{\sigma^2}{2}}$. The continuous lines in Figure 5, show such fits. Log–log plot of $\langle R \rangle$ in term of film thickness (that is shown in Figure 5) is a straight line so that $\langle R \rangle$ scales as:

$$\langle R \rangle \sim t^{1/z} \quad (4)$$

Where z is the dynamic exponent. The gradient of the fitted line to data of this figure gives the $1/z$ =0.63$\pm$0.07. This value is consistent with value determined in our previous work, which was determined by atomic force microscopy analysis [26]. The high value obtained here for 1/z also indicates mound coarsening on the surface [27].

The exponent of z is a characteristic growth exponent whose value depends on the specific properties of the growth process. According to the references [28, 29], for the three-dimensional cluster growth with only the contact line to the substrate surface active in mass transport, the critical radius of the clusters will grow with a dynamic exponent 1/z = 1/3; if, instead, for the three-dimensional clusters the full cluster surface is active in mass transport, a dynamic exponent 1/z = 1/2 is expected.

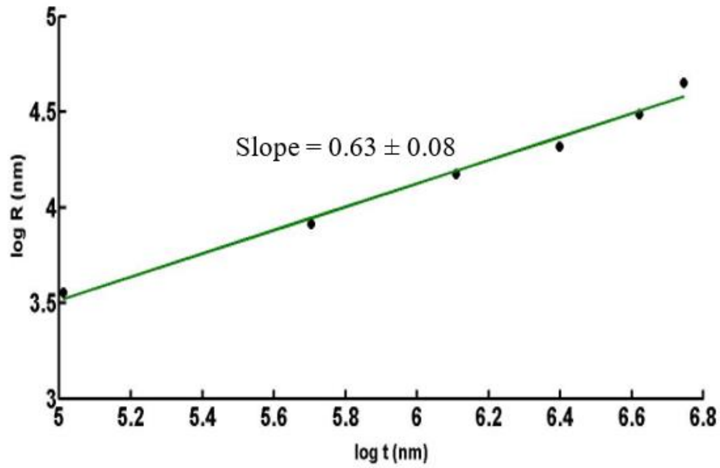

Fig 6. Log–log plot of mean radius of the grains in term of film thickness.

The value of 1/z = 0.63 ± 0.08 obtained in the present experiment, is suggested that a three dimensional cluster growth in which the full cluster surface rather than the contact line to the substrate surface is active in the mass transport. Now we compare the data presented in this study with other experimental works. The value of 1/*z*= 0.63 ± 0.08 and β=0.69± 0.08 obtained in the present study is comparable to that reported by Dharmadhikari et al. for Pt films on Si (100) 1/*z*=0.71 and β=0.52 [30] and to that reported by Xu et al. for electrodeposited PdNiP on Au 1/*z*=1.1 and β=0.66 [31]. X-ray specular reflectivity in term of q_z (that is equal to $4\pi sin\theta/\lambda$ and is called wave transfer vector perpendicular to the surface) for some samples (electrodeposited on the Cu substrate) are reported in figure 7. According to the reference [30], the oscillations in the data arise from the interference between the portion of the beam reflected from the film–vacuum (air) interface and the substrate–film interface, and the curves are decaying with increase in the film thickness. In the reflectivity curves, the oscillation is observed near $q_z = 0.1\,A^{-1}$ which is because of the total thickness of Ag film. Also, there are rapid fall of reflectivity after q_c (critical wave vector, showed by an arrow in the reflectivity curves) and the damping of the oscillation indicating high roughness at surface of the Ag films. Roughness gives rise to diffuse scattering, resulting to a less intensity in the specularly reflected beam. Hence, it is found that surface roughness increased with increasing thickness. According to the reference [13],The rise of surface roughness caused that surface of Ag samples became more hydrophilic. This property is very important for antibacterial activity of silver nanolayers in removal of E. coli. Although the mechanisms behind this activity of nanoscaled Ag on bacteria are not yet fully elucidated, but the most common mechanism behind this activity are proposed to date are uptake of free Ag ions followed by disruption of adenosine triphosphate production and deoxyribonucleic acid replication and also Ag nanoparticles and its ions generation of reactive oxygen species [32].

Table 1. The values of film thickness, density, critical wave vector of the Ag films.

t(nm)	ρ(g/ cm^3)	$q_c(A^{-1})$
300	9.15	0.04
450	9.35	0.045
750	9.81	0.05

As the grain size in silver thin films increases, the specific surface area decreases due to a reduced number of active sites available for the release of silver ions (Ag^+). This reduction can lead to a lower ion release rate and consequently diminished antibacterial activity. On the other hand, an increase in surface roughness results in a larger total surface area, which partially compensates for the loss of specific surface area caused by grain growth. Higher roughness also enhances the contact and distribution of silver ions in the surrounding environment and facilitates mass transfer, thereby improving antimicrobial efficacy. Moreover, larger grains generally form a denser structure with better adhesion to the substrate, which enhances the mechanical stability of the thin film and reduces its degradation rate under operational conditions. Therefore, with increasing thickness of silver thin films, a balance is established between the reduced ion release rate due to grain growth and the improved antimicrobial performance resulting from increased surface roughness, ultimately leading to more stable antibacterial activity and enhanced film durability.
The density (ρ) was calculated from the value of θ_c (the critical angle for total reflection) using the relation [33]:

$$\theta_c^{\,2} = 5.402 \times 10^{-6} \rho \lambda^2 (Z + \acute{f})/A \quad (5)$$

Where A and Z are the atomic weight and the atomic number, respectively. Moreover, $\acute{f}$ is the real part of the anomalous dispersion correction. The values of density of the Ag films obtained from the specular reflectivity curve are listed in table 1. It can be found that these values are less than the 10.49 g/ cm^3 value for bulk Ag. This result in agreement with that reported by Huang and et al for Pt films [20]. The reduction in density of the Ag film was probably caused by a very thin layer of oxygen contaminating the surface of the Ag film [21]. Also, it was probably attributed to the presence of the voids in the islands along with the low connectivity of the islands. Reduction of density in nanocrystalline Ag was found earlier [22]. As the grains grow with the deposition time the connectivity in x-y plane increases and hence the density of the layers increases. It is in agreement with similar studies [34].

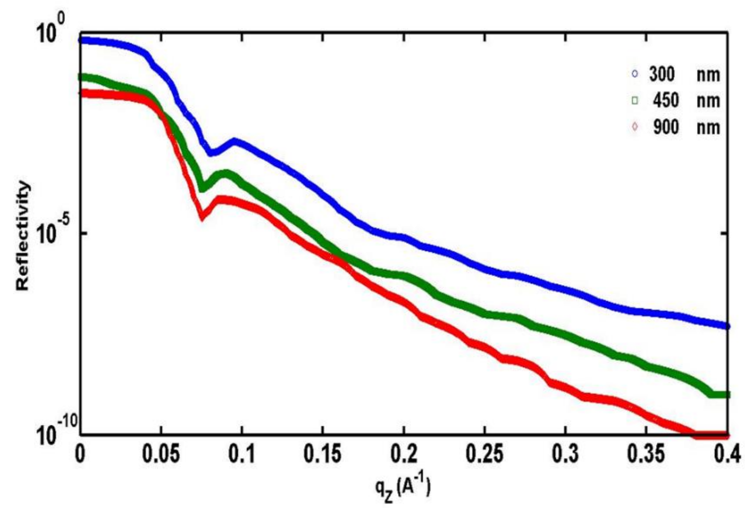

Fig 7. X-ray specular reflectivity for Ag films with the different thickness.

4. Conclusion

In this study, the morphological, structural, and antibacterial properties of electrodeposited silver (Ag) thin films were investigated with an emphasis on substrate type and film thickness. The results clearly demonstrate that substrate material plays a critical role in determining the surface morphology and structural integrity of the films, which directly impacts their antibacterial performance. Films deposited on Cu substrates exhibited a granular and compact morphology conducive to a stable and uniform release of silver ions, while those on Au_2PdAg/glass showed surface cracks that could compromise their functionality.
XRD analysis confirmed the polycrystalline nature of the films with a preferred (111) orientation, enhancing the surface activity and promoting efficient Ag^+ ion release. The crystallite size followed the dynamic scaling law with a growth exponent $\beta = 0.67$, indicative of anomalous roughness evolution due to non-local effects such as bulk diffusion.

SEM and grain distribution analyses revealed that increased film thickness led to larger grain sizes and higher surface roughness, both of which influenced the ion release behavior and film durability. The analyses of the SEM images of the Ag thin film with respect to film thickness (or deposition time) allowed us to extract the dependence of the silver grain size on the film thickness. The value of $1/z = 0.63 \pm 0.07$ obtained in the present experiment, is suggested that a three dimensional cluster growth in which the full cluster surface rather than the contact line to the substrate surface is active in the mass transport.
Furthermore, X-ray reflectivity measurements revealed an increasing roughness roughness with increased thickness. The increased roughness was found to enhance hydrophilicity, which is favorable for antibacterial activity. Despite a reduction in specific surface area with grain growth, the increased roughness compensated for this effect, resulting in sustained antimicrobial efficacy.
Overall, the interplay between grain size, surface roughness, and substrate-film interactions must be carefully balanced to optimize the antibacterial performance and durability of Ag thin films in water and wastewater treatment applications. These findings offer valuable insights for the rational design and engineering of advanced antibacterial coatings. The values of density of the Ag films obtained from the specular reflectivity curve show that their values are less than the 10.49 g/ cm3 value for bulk Ag.

Conflict-of-interest: The author declares no conflict of interest

Funding: No funding was received for conducting this study.

References

[1] A. Naseri, M. Goodarzi, D. Ghanbari. ,Green synthesis and characterization of magnetic and effective photocatalyst $NiFe_2O_4$–NiO nanocomposites., Journal of Materials Science: Materials in Electronics 28 (2017) 17635-17646. https://doi.org/10.1007/s10854-017-7702-z
[2] K. Hedayati, Structural and magnetic characterization of electrodeposited Ni–Cu/Cu and Fe–Ni–Cu/Cu multilayer., Applied Physics A 118 (2015) 975-979. https://doi.org/10.1007/s00339-014-8851-z
[3] C-C. Chang, L-Y. Chen, K-H. Yang, Q-Y. Chen, Y-C. Liang, S-Y. Lin, Y-C. Liu, Surface-enhanced Raman scattering on a silver film-modified Au nanoparticle-decorated SiO2 mask array, RSC advances 5, no. 81 (2015) 66096-66103. https://doi.org/10.1039/C5RA11183H
[4] Z-Q. Cheng, Z-W. Li, J-H. Xu, R Yao, Z-L Li, S. Liang, G-L. Cheng, Y-H. Zhou, X. Luo, J. Zhong, Morphology-controlled fabrication of large-scale dendritic silver nanostructures for catalysis and SERS applications, Nanoscale Research Letters 14 (2019) 1-7. https://doi.org/10.1186/s11671-019-2923-0
[5] G. Wang, C. Wang, R. Yang, W. Liu, Sh. Sun, A sensitive and stable surface plasmon resonance sensor based on monolayer protected silver film, Sensors 17 (2017) 2777. https://doi.org/10.3390/s17122777
[6] C. Zhang, N. Kinsey, L. Chen, Ch. Ji, M. Xu, M. Ferrera, X. Pan, V M. Shalaev, A. Boltasseva, and L. Jay Guo, High-performance doped silver films: overcoming fundamental material limits for nanophotonic applications, Advanced Materials 29 (2017) 1605177. https://doi.org/10.1002/adma.201605177
[7] Y. Lu, Ch.Wu, R. You, Y. Wu, H. Shen, L. Zhu, Sh. Feng, Superhydrophobic silver film as a SERS substrate for the detection of uric acid and creatinine, Biomedical Optics Express 9 (2018): 4988-4997. https://doi.org/10.1364/BOE.9.004988
[8] R. Veera Babu, Jean Maria Fernandes, M. Kovendhan, Nandarapu Purushothamreddy, Reddivari Muniramaiah, R. Arockiakumar, N.S. Karthiselva, D. Paul Joseph, Investigation of structural, optical, electrical and mechanical properties of transparent conducting 'Ag' electrodes, Physica B: Physics of Condensed Matter 607 (2021) 412690. https://doi.org/10.1016/j.physb.2020.412690
[9] R. Haji Abdolvahab, M.R. Zamani Meymian, Theoretical and experimental analyses of the deposited silver thin films, Surface and Interface Analysis 50 (2018) 403-410. https://doi.org/10.1002/sia.6381
[10] X. Zhang, and M. Kobayashi, Study on growth process of Ag (In, Ga) Se2 films by a three-stage co-evaporation method using molecular beam epitaxy apparatus, IEEE Photonics Journal 9 (2017) 1-9. https://doi.org/10.1109/JPHOT.2017.2670923
[11] Nikolay N. Durmanov, Rustam R. Guliev, Arkady V. Eremenko, Irina A. Boginskaya, Ilya A. Ryzhikov, Ekaterina A. Trifonova, Egor V. Putlyaev et al, Non-labeled selective virus detection with novel SERS-active porous silver nanofilms fabricated by Electron Beam Physical Vapor Deposition, Sensors and Actuators B: Chemical 257 (2018) 37-47. https://doi.org/10.1016/j.snb.2017.10.022
[12] M. Nasehnejad, Gh. Nabiyouni, M. Gholipour Shahraki, Morphological characterisation and microstructure of silver films prepared by electrodeposition method, Surface Engineering 33 (2017) 389-394. https://doi.org/10.1080/02670844.2016.1277631
[13] A. Zendehnam, J. Ghasemi, A. Zendehnam, Employing cold atmospheric plasma (Ar, He) on Ag thin film and their influences on surface morphology and anti-bacterial activity of silver films for water treatment, International Nano Letters 8 (2018) 157-164. https://doi.org/10.1007/s40089-018-0240-8

[14] D. Aydin, İ. H. Gübbük, M. Ersöz, Recent advances and applications of nanostructured membranes in water purification, Turkish Journal of Chemistry 48, no. 1 (2024) 1-20.

[15] Z-K. Tan, J-L. Gong, S-Y. Fang, J. Li, W-C. Cao, Z-P. Chen. , Outstanding anti-bacterial thin-film composite membrane prepared by incorporating silver-based metal–organic framework (Ag-MOF) for water treatment, Applied Surface Science 590 (2022) 153059. https://doi.org/10.1016/j.apsusc.2022.153059

[16] H. Yu, H. Zhang, C. Zhang, R. Wang, S. Liu, R. Du, W. Sun, Advances in treatment technologies for silver-containing wastewater, Chemical Engineering Journal (2024) 153689. https://doi.org/10.1016/j.cej.2024.153689

[17] H. Kuruva, V. B. Khavala, B. R. Mishra, K. Murugan, Tiju Thomas, B. S. Murty, Enhancing photocatalytic efficiency and durability: Ag-modified CNS–TiO_2 thin films for sustainable industrial wastewater treatment, Optical Materials 150 (2024) 115180. https://doi.org/10.1016/j.optmat.2024.115180

[18] G. Nabiyouni, M. Nasehnejad, Conventional and fractal analyses and nanoscale behavior studies of electrodeposited silver films, Physica B: Condensed Matter 548 (2018) 46-52. https://doi.org/10.1016/j.physb.2018.08.014

[19] M. Nasehnejad, G. Nabiyouni., Role of Substrate on the Fractal Characteristics of Nanostructure Surfaces of Electrodeposited Nickel Thin Films, physica status solidi (b) 261, no. 8 (2024): 2400109. https://doi.org/10.1002/pssb.202400109

[20] T. C. Huang, R. Giiles and G. Will, Thin-film thickness and density determination from X-ray reflectivity data using a conventional power diffractometer, Thin Solid Films, 230 (1993)99-101. https://doi.org/10.1016/0040-6090(93)90499-F

[21] T. C. Huang, Grazing-incidence X-ray analysis of surfaces and thin films, Advances in X-Ray Analysis 35 (1991): 143-150. https://doi.org/10.1154/S0376030800008776

[22] T. Kizuka, Y. Nakagami, T. Ohata, I. Kanazawa, H. Ichinose, H.Murakami, Y. Ishida, Structure and thermal stability of nanocrystalline silver studied by transmission electron microscopy and positron annihilation spectroscopy, Philosophical Magazine A 69 (1994) 551-563. https://doi.org/10.1080/01418619408242229

[23] M. Nasehnejad, G. Nabiyouni, M. Gholipour Shahrakim, Dynamic scaling study of nanostructured silver films, Journal of Physics D: Applied Physics 50, no. 37 (2017) 375301. http://dx.doi.org/10.1088/1361-6463/aa7d78

[24] F. Ruffino, A. Irrera, R. De Bastiani, M. G. Grimaldi, Room-temperature grain growth in sputtered nanoscale Pd thin films: Dynamic scaling behaviour on SiO_2, Journal of Applied Physics 106 (2009) 084309. https://doi.org/10.1063/1.3246619

[25] C. G. Granqvist, R. A. Buhrman, Ultrafine metal particles, Journal of applied Physics 47 (1976) 2200-2219. https://doi.org/10.1063/1.322870

[26] M. Nasehnejad, G. Nabiyouni, M. Gholipour Shahraki Atomic force microscopy study, kinetic roughening and multifractal analysis of electrodeposited silver films." Applied Surface Science 389 (2016): 735-741.https://doi.org/10.1016/j.apsusc.2016.07.134

[27] G. Zhang, B. L. Weeks, M. Holtz, Application of dynamic scaling to the surface properties of organic thin films: Energetic materials, Surface science 605 (2011) 463-467. https://doi.org/10.1016/j.susc.2010.11.018

[28] M. Zinke-Allmang, L.C. Feldman, M.H. Grabov, Clustering on surfaces, Surf. Sci.Rep. 16 (1992) 377–463. https://doi.org/10.1016/0167-5729(92)90006-W

[29] F. Ruffino, V. Torrisi, G. Marletta, M.G. Grimaldi, Atomic force microscopy investigation of the kinetic growth mechanisms of sputtered nanostructured Au film on mica: towards a nanoscale morphology control, Nanoscale Res. Lett. 6 (2011) 1–13. https://doi.org/10.1186/1556-276X-6-112

[30] C.V. Dharmadhikaria, A.O. Alia, N. Sureshb, D.M. Phaseb, S.M. Chaudharib, V. Ganesanb, A. Guptab, B.A. Dasannacharyab, Dynamic scaling in growth of platinum films on Si (100), Solid State Commun. 114 (2000) 377–381. https://doi.org/10.1016/S0038-1098(00)00069-7

[31] Y. Xu, X-M. Ge, Y-J. Tong, H-L. Xie, T-Q. Xiao, J-Z. Jiang. , Kinetic surface roughening of electrodeposited amorphous PdP and NiP films–A comparative study, Electrochemistry communications 12 (2010): 442-445. https://doi.org/10.1016/j.elecom.2010.01.015

[32] J.L. Ramos, Virulence and gene regulation. Springer, Berlin (2012)

[33] R. Feidenhans, Surface structure determination by X-ray diffraction, , Surf Sci. Rep. 10 (1989) 105. https://doi.org/10.1016/0167-5729(89)90002-2

[34] S. Kundu, S. Hazra, S. Banerjee, M. K. Sanyal, S. K. Mandal, S. Chaudhuri, A. K. Pal, Morphology of thin silver film grown by dc sputtering on Si (001), Journal of Physics D: Applied Physics 31, (1998) L73. https://doi.org/10.1088/0022-3727/31/23/001/meta